

An XMCD-PEEM study on magnetized Dy-doped Nd-Fe-B permanent magnets

R. Yamaguchi
K. Terashima
K. Fukumoto
Y. Takada
M. Kotsugi
Y. Miyata
K. Mima
S. Komori
S. Itoda
Y. Nakatsu
M. Yano
N. Miyamoto
T. Nakamura
T. Kinoshita
Y. Watanabe
A. Manabe
S. Suga
S. Imada

We have succeeded in developing a method for photoemission electron microscopy (PEEM) on fully magnetized ferromagnetic bulk samples and have applied this technique to Dy-doped Nd-Fe-B permanent magnets. Remanence magnetization of the sample was approximately 1.2 T, and its dimension was $3 \times 3 \times 3 \text{ mm}^3$. By utilizing a yoke as an absorber of the stray magnetic field from the sample, we can obtain well-focused PEEM images of magnetized samples. We have observed not only chemical distributions to visualize Dy-rich and Dy-poor areas but also magnetic domains by x-ray magnetic circular dichroism. The formation of reversed magnetic domains is strongly suppressed at room temperature by Dy-doping. As the temperature of the Dy-doped sample is raised, starting from room temperature, the reversed magnetic domains first grow along the magnetization easy axis. Next, above approximately 80°C , the shapes of reversed domains start to expand in the direction perpendicular to the easy axis. Above approximately 85°C , the reversed domains cover more than half of the field of view of $30 \mu\text{m}$. More importantly, the reversed magnetic domains tend to nucleate or extend in Dy-poor regions. We discuss the relationship between the chemical distribution and the magnetic domain structure.

Introduction

Nd-Fe-B permanent magnets, which were invented more than 25 years ago [1], have the largest magnetic energy integral and have been widely used. For their application to propulsion electric motors on hybrid vehicles, resistivity to heat is indispensable. A pristine Nd-Fe-B magnet is seriously vulnerable to heat. For example, magnetization irreversibly decreases to half already at about 130°C . The present solution to this problem is to partly replace Nd with Dy. By Dy doping, thermal demagnetization is strongly suppressed, and temperature dependence becomes nearly reversible. At the same time, coercivity strongly increases. Since Dy is much scarcer than Nd, an inexpensive substitute is highly desired. Therefore, it is important to clarify not only the effect of Dy to the magnetic property but also its detailed mechanism.

There have been intensive studies of Nd-Fe-B magnets from both fundamental and application points of view [2–4]. Research using methods such as Kerr microscope methods has revealed that magnetic domain structures, particularly the reversed magnetic domains, play the central role in thermal demagnetization of Nd-Fe-B [5]. In addition, it has been shown that metallographic structures in the micrometer and nanometer ranges of phases such as the mother $\text{Nd}_2\text{Fe}_{14}\text{B}$ phase and B- or Nd-rich phases are important.

In order to determine the effects of Dy on Nd-Fe-B magnets, we need to clarify the chemical distribution of the doped Dy and its relationship to the reversed magnetic domains. Photoemission electron microscopy (PEEM) can be used to observe the spatial element distribution on the surface of a sample through use of x-ray photoabsorption edges. Combination with the x-ray magnetic circular dichroism (XMCD) enables one to observe magnetic domain structures on the same surface [6–8]. This method, i.e., XMCD-PEEM, is one of the most relevant tools for determining the effect

Digital Object Identifier: 10.1147/JRD.2011.2159148

© Copyright 2011 by International Business Machines Corporation. Copying in printed form for private use is permitted without payment of royalty provided that (1) each reproduction is done without alteration and (2) the Journal reference and IBM copyright notice are included on the first page. The title and abstract, but no other portions, of this paper may be copied by any means or distributed royalty free without further permission by computer-based and other information-service systems. Permission to republish any other portion of this paper must be obtained from the Editor.

0018-8646/11/\$5.00 © 2011 IBM

Table 1 Concentration in unit of mass percentage of the measured samples of the undoped and Dy-doped Nd-Fe-B permanent magnets.

	<i>Dy</i>	<i>Nd</i>	<i>Tb</i>	<i>Co</i>	<i>Al</i>	<i>Cu</i>	<i>B</i>	<i>Fe</i>
<i>Undoped</i>	—	29.2	—	0.09	0.33	0.18	0.97	Remainder
<i>Dy doped</i>	4.7	24.0	0.75	2.04	0.35	0.21	1.00	Remainder

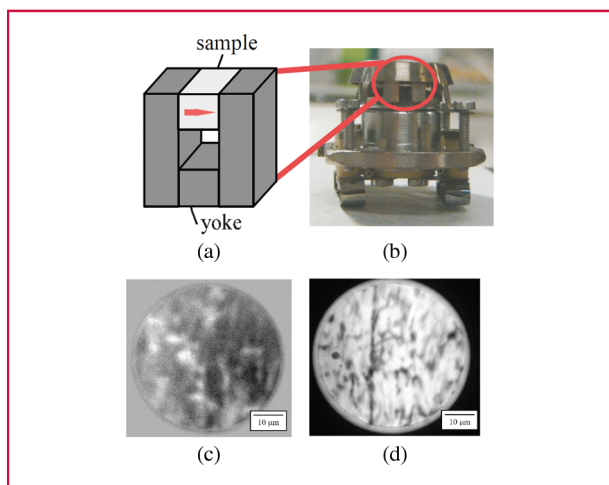


Figure 1

Yoke systems and results. (a) Sketch of the yoke system to absorb the stray field from the permanent-magnet sample. The red arrow indicates the direction of magnetization. (b) The yoke system attached on an Elmitec PEEM sample holder. (c) and (d) Examples of XMCD-PEEM images taken by the setup with (c) a large residual stray field and with (d) a sufficiently small stray field. The magnetization direction is in the plane of the surface of the sample and is parallel to the vertical axis of the figure. The reversed domains are shown in dark and light shades in (c) and (d), respectively.

of the concentration distribution of Dy on the performance of the Nd-Fe-B permanent magnet [9]. Since the reversed magnetic domains are thought to emerge first on the surface of magnets, the surface sensitivity of XMCD-PEEM is also advantageous.

Until now, PEEM measurement of magnetized bulk materials has not been possible because the trajectories of photoelectrons are bent by the stray magnetic field from the sample. Therefore, Nd-Fe-B magnets have been demagnetized, either by heating or by applying an alternating-current magnetic field, in advance to the PEEM observation [9]. We have solved this problem by using a soft magnetic yoke to make the stray magnetic field be absorbed and have succeeded in the XMCD-PEEM measurement of fully magnetized Dy-doped Nd-Fe-B magnets. In this paper, we first report the method to enable

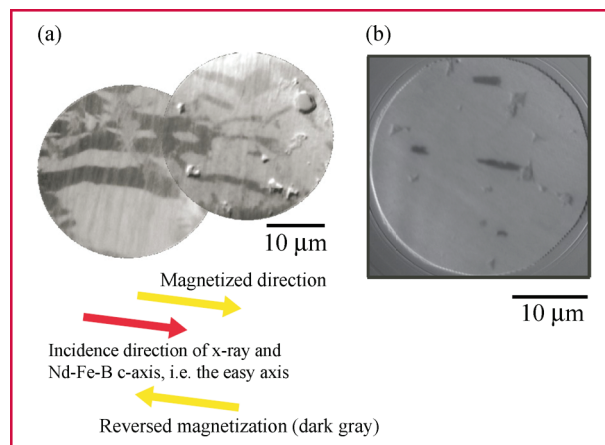


Figure 2

Magnetic domain structures observed at room temperature with XMCD-PEEM at the Fe L_3 edge for the (a) undoped and (b) Dy-doped Nd-Fe-B permanent-magnet surfaces with the field of view of $30 \mu\text{m}$.

PEEM observation of fully magnetized magnets. Next, we present the observed chemical contrast and magnetic domain structures on the surface of a Dy-doped Nd-Fe-B magnet. Based on these results, we discuss the role of Dy in the performance of Nd-Fe-B magnets.

Experimental method

We have measured a Nd-Fe-B magnet without Dy doping (undoped) and a Dy-doped one with the chemical concentrations shown in **Table 1**. The samples were magnetized using a magnetic field of 10 T and then cut and attached to a soft magnetic yoke, as explained below. XMCD-PEEM measurements were performed using two different setups at the SPring-8 facility in Japan, namely, Elmitec PEEM-SPECTOR at the BL-25SU beamline and Elmitec spectroscopic low-energy electron microscope (SPELEEM) at the BL-17SU beamline. The test of the yoke system, the results of which are shown in **Figure 1**, was performed using the former setup. The main part of the study on permanent magnets, the results of which are shown in **Figures 2–4**, was performed using the latter setup. The electron energy filter equipped in SPELEEM enables higher

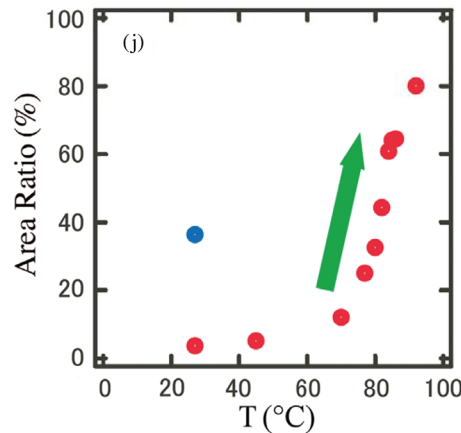
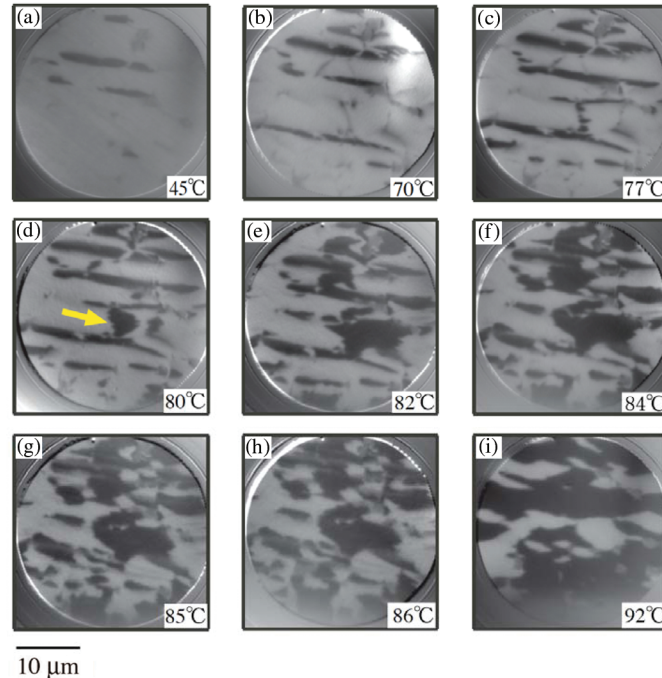


Figure 3

Temperature dependence of reversal domains. (a)–(i) Temperature dependence of the magnetic domain structure on the surface of the Dy-doped Nd-Fe-B permanent magnet upon heating measured by XMCD-PEEM at the Fe L_3 edge with the field of view of $30 \mu\text{m}$. (j) Temperature dependence of the area ratio of the reversed domains calculated from (a)–(i) (red dots) together with that for the undoped Nd-Fe-B permanent magnet at room temperature (blue dot).

spatial resolution by preventing the energy aberration induced by the wide energy distribution of photoelectrons excited by soft x-rays. Magnetic domain structures were observed using soft x-rays corresponding to the L_3 (i.e., $2p_{3/2} \rightarrow 3d$) photoabsorption peak of Fe and by changing the circular polarization. Magnetic contrast was obtained by calculating the difference between the images for the two opposite circular polarizations. Chemical distributions of Fe and Dy have been measured at the Fe L_3

and Dy M_5 (i.e., $3d_{5/2} \rightarrow 4f$) absorption edges. Chemical contrast was obtained by calculating the ratio between the image taken at the absorption peak and that taken before the edge. The temperature of the Dy-doped sample was elevated, starting from room temperature, in order to study the thermal demagnetization process.

In order to make the stray magnetic field be absorbed, samples have been attached without a gap to a soft magnetic yoke made of pure iron, as shown in Figure 1(a). However,

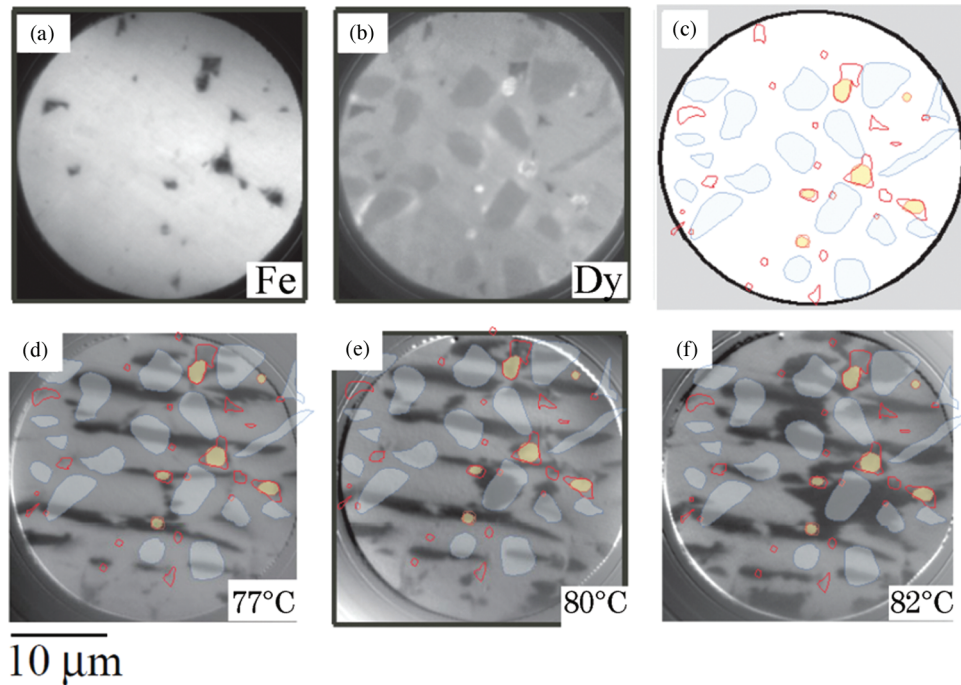


Figure 4

Comparison between the chemical and magnetic structures of the Dy-doped Nd-Fe-B permanent magnet with the field of view of $30\ \mu\text{m}$. (a) Fe distribution measured by PEEM at the Fe L_3 edge. (b) Dy distribution measured at the Dy M_5 edge. (c) Sketch of (red) the triple points and (yellow) the Dy-rich and (blue) Dy-poor regions based on (a) and (b). (d)–(f) Sketch (c) superimposed on the temperature-dependent magnetic domain structures measured by XMCD-PEEM at the Fe L_3 edge.

this procedure does not necessarily lead to a good focus of the PEEM image. There was a strong correlation between the focus and the stray magnetic field near the surface of the sample, which is measured by a Gauss meter. When the stray magnetic field of 8 mT was still present, the PEEM image did not focus well [see Figure 1(c)]. The stray field was strongest near the junctions between the sample and the yoke. In order to suppress the stray magnetic field sufficiently, we have (1) carefully shaped the sample so that the four surfaces, which are not in contact with the yoke, are accurately parallel to the magnetization direction, being the

c -axis of the $(\text{Nd}_{1-x}\text{Dy}_x)_2\text{Fe}_{14}\text{B}$ mother phase particles in the sample and (2) carefully aligned the surfaces of the sample and the yoke to the same height in order to avoid any step at the junction. When the stray field was reduced to less than 1 mT by this method, the PEEM image focused well, as shown in Figure 1(d).

Results and discussion

Magnetic domain structures of the undoped and the Dy-doped samples, which are observed by XMCD-PEEM at room temperature, are shown in Figure 2(a) and 2(b),

respectively. The red arrow shows the direction of the incident circularly polarized x-ray. The yellow arrows show the direction of the samples' magnetization and reversed magnetization. In the XMCD-PEEM images, the lighter and darker parts are magnetized in the former and the latter directions, respectively. In the undoped sample, many reversed magnetic domains are found. In the Dy-doped sample, on the other hand, reversed domains are drastically suppressed. In both samples, the shapes of the reversed magnetic domains tend to be longer in the direction of the easy magnetization axis.

Figure 3(a)–3(i) show the observed temperature dependence of the magnetic domain structure of the Dy-doped sample upon heating from room temperature to approximately 90°C. We have calculated the area ratio of the reversed domains in the field of view and have shown its temperature dependence in Figure 3(j). At room temperature, the reversed domains already amount to approximately 40% in the case of the undoped sample, whereas the amount is suppressed to less than 10% in the Dy-doped sample. Even in the Dy-doped sample, the reversed domains on the surface clearly increase both in numbers and in area by heating. Up to about 70°C, the reversed magnetic domains tend to grow in the direction parallel to the easy magnetization axis. However, their shapes expand in the direction perpendicular to the easy magnetization axis above approximately 80°C, leading to much wider shapes of the reversed domains [see, for example, the area indicated by a yellow arrow in Figure 3(d)]. This suggests that, in this temperature range, the hard magnetization axis is not hard enough to keep the reversed domains' shape narrow and long along the *c*-axis. The reason might be that a characteristic energy value related to the magnetic anisotropy field decreases upon heating [2–4] and becomes comparable to $k_B T$ in this temperature range, where k_B is Boltzmann's constant. In the same temperature range, the area of the reversed domains drastically increases, as illustrated by the green arrow in Figure 3(j). This indicates that the rapid growth of the reversed domains is also induced because the magnetic anisotropy energy decreases upon heating. At 92°C, the reversed magnetic domains occupy much more than half of the whole area. This is interpreted as such because the magnetic field emitted by the bulk of the sample, which is still strongly magnetized even at 92°C, partly runs on the surface of the sample in the opposite direction as the bulk instead of running in the yoke. The reason for this is that the length of the line of the magnetic field is shorter when it passes on the surface of the sample than when it goes through the yoke.

Next, we compare the magnetic domain structures with the chemical distribution in Figure 4. Figure 4(a) and 4(b) show the chemical distribution of Fe and Dy, respectively, where lighter color corresponds to larger concentration. The black points in Figure 4(a) are the “triple points,” at

which three grain boundaries meet. Therefore, a grain boundary (i.e., a boundary between different grains of mother composition) is expected to run from a triple point to another. Since many triple points are too small to be seen in this figure, one cannot draw grain boundaries by relying only on the Fe distribution. In Figure 4(c), the positions of the triple points are superimposed on the chemical contrasts of Fe and Dy. Yellow areas show the Dy-rich regions, and blue areas show the Dy-poor regions. The red lines show the triple points. In Figure 4(d)–4(f), the sketch in Figure 4(c) is superimposed on top of the magnetic domain structure at 77°C, 80°C, and 82°C, respectively. The reversed magnetic domains tend to rapidly grow near the Dy-poor regions. In particular, wider domains, which appear at 80°C and 82°C, are all located in the vicinity of the Dy-poor regions.

Dy doping is known to enhance the magnetic anisotropy of a Nd-Fe-B magnet [2, 3]. The Dy-poor parts have smaller magnetic anisotropy; therefore, the energy barrier against the rotation of the magnetization direction is lower, leading to easier growth of the reversed domains. At approximately 80°C, the magnetic anisotropy of the Dy-poor parts becomes small enough for the shapes of the reversed domains to expand in the direction perpendicular to the magnetization easy axis, leading to the rapid growth of the total area of the reversed domains.

Conclusion

We have succeeded in observing the temperature dependence of the magnetic domains of fully magnetized Nd-Fe-B permanent magnets using XMCD-PEEM. This has been realized by absorbing the stray magnetic field with use of a soft magnetic yoke. We have observed the change of the magnetic domain structure, particularly the growth of the reversed domains, upon heating from room temperature to about 90°C. Up to about 70°C, the reversed domains grow along the *c*-axis, and the growth is gradual. Above approximately 80°C, rapid growth is observed, and the reversed domains become wider, i.e., their shapes expand in the direction perpendicular to the *c*-axis. We have compared the magnetic domain structure with the chemical distribution of Fe and Dy. The reversed domains tend to grow near the Dy-poor parts in the sample, which is consistent with the discussion that Dy doping enhances magnetic anisotropy.

Acknowledgments

Synchrotron radiation experiments in SPring-8 have been performed with the approval of Japan Synchrotron Radiation Research Institute (Proposal Number 2007A1884 at BL-25SU; Proposal Numbers 2007B1838, 2008A1838, and 2008B1954 at BL-17SU).

References

1. M. Sagawa, S. Fujimura, N. Togawa, H. Yamamoto, and Y. Matsuura, “New material for permanent magnets on a base of Nd and Fe,” *J. Appl. Phys.*, vol. 55, no. 6, pp. 2083–2087, Mar. 1984.

2. S. Hirose, Y. Matsuura, H. Yamamoto, S. Fujimura, and M. Sagawa, "Magnetization and magnetic anisotropy of $R_2Fe_{14}B$ measured on single crystals," *J. Appl. Phys.*, vol. 59, no. 3, pp. 873–879, Feb. 1986.
3. M. Sagawa, S. Hirose, K. Tokuhara, H. Yamamoto, and S. Fujimura, "Dependence of coercivity on the anisotropy field in the $Nd_2Fe_{14}B$ -type sintered magnets," *J. Appl. Phys.*, vol. 61, no. 8, pp. 3559–3561, Apr. 1987.
4. J. F. Herbst, " $R_2Fe_{14}B$ materials: Intrinsic properties and technological aspects," *Rev. Mod. Phys.*, vol. 63, no. 4, pp. 819–898, Oct.–Dec. 1991.
5. A. Hubert and R. Schäfer, *Magnetic Domains; The Analysis of Magnetic Microstructures*. Berlin, Germany: Springer-Verlag, 1998.
6. J. Stöhr, Y. Wu, D. Hermsmeier, M. G. Samant, G. R. Harp, S. Koranda, D. Dunham, and B. P. Tonner, "Element-specific magnetic microscopy with circularly polarized x-rays," *Science*, vol. 259, no. 5095, pp. 658–661, 1993, Reprint Series.
7. T. Kinoshita, "Application and future of photoelectron spectromicroscopy," *J. Electron Spectrosc. Relat. Phenom.*, vol. 124, no. 2/3, pp. 175–194, Jul. 2002.
8. S. Imada, S. Suga, W. Kuch, and J. Kirschner, "Magnetic microspectroscopy by a combination of XMCD and PEEM," *Surf. Rev. Lett.*, vol. 9, no. 2, pp. 877–881, 2002.
9. S. Yamamoto, M. Yonemura, T. Wakita, K. Fukumoto, T. Nakamura, T. Kinoshita, Y. Watanabe, F. Z. Guo, M. Sato, T. Terai, and T. Kakeshita, "Magnetic-domain structure analysis of Nd-Fe-B sintered magnets using XMCD-PEEM technique," *Mater. Trans.*, vol. 49, no. 10, pp. 2354–2359, 2008.

Received October 1, 2010; accepted February 14, 2011

Ryosuke Yamaguchi *Department of Physical Sciences, Ritsumeikan University, Kusatsu, Shiga 525-8577, Japan.*

Kensei Terashima *Department of Physical Sciences, Ritsumeikan University, Kusatsu, Shiga 525-8577, Japan (kterashi@fc.ritsumei.ac.jp).*

Keiki Fukumoto *Japan Synchrotron Radiation Research Institute (JASRI), Sayo, Hyogo 679-5198, Japan; Toyota Central Research & Development Laboratories, Inc., Nagakute, Aichi 480-1192, Japan; Department of Materials Science, Tokyo Institute of Technology, Meguro-ku, Tokyo, 152-8550, Japan (fukumoto.k.ab@m.titech.ac.jp).*

Yukio Takada *Toyota Central Research & Development Laboratories, Inc., Nagakute, Aichi 480-1192, Japan.*

Masato Kotsugi *Japan Synchrotron Radiation Research Institute (JASRI), Sayo, Hyogo 679-5198, Japan (kotsugi@spring8.or.jp).*

Yuta Miyata *Department of Physical Sciences, Ritsumeikan University, Kusatsu, Shiga 525-8577, Japan.*

Kazuma Mima *Department of Physical Sciences, Ritsumeikan University, Kusatsu, Shiga 525-8577, Japan.*

Satoshi Komori *Department of Materials Physics, Osaka University, Toyonaka, Osaka 560-8531, Japan; Toyota Motor Corporation, Toyota, Aichi 471-8571, Japan.*

Shuichi Itoda *Department of Materials Physics, Osaka University, Toyonaka, Osaka 560-8531, Japan.*

Yoshitaka Nakatsu *Department of Materials Physics, Osaka University, Toyonaka, Osaka 560-8531, Japan.*

Masao Yano *Department of Materials Physics, Osaka University, Toyonaka, Osaka 560-8531, Japan; Toyota Motor Corporation, Toyota, Aichi 471-8571, Japan (yano@masao.tec.toyota.co.jp).*

Noritaka Miyamoto *Toyota Motor Corporation, Toyota, Aichi 471-8571, Japan.*

Tetsuya Nakamura *Japan Synchrotron Radiation Research Institute (JASRI), Sayo, Hyogo 679-5198, Japan (naka@spring8.or.jp).*

Toyohiko Kinoshita *Japan Synchrotron Radiation Research Institute (JASRI), Sayo, Hyogo 679-5198, Japan (toyohiko@spring8.or.jp).*

Yoshio Watanabe *Japan Synchrotron Radiation Research Institute (JASRI), Sayo, Hyogo 679-5198, Japan (watanabe@ncassembly.jst.go.jp).*

Akira Manabe *Toyota Motor Corporation, Toyota, Aichi 471-8571, Japan.*

Shigemasa Suga *Department of Materials Physics, Osaka University, Toyonaka, Osaka 560-8531, Japan (ssmsuga@gmail.com).*

Shin Imada *Department of Materials Physics, Osaka University, Toyonaka, Osaka 560-8531, Japan; Department of Physical Sciences, Ritsumeikan University, Kusatsu, Shiga 525-8577, Japan (imada@se.ritsumei.ac.jp).*